

Preliminary test results of cruciform test specimens

OB_TG2_R007_VUB rev. 000

Draft version
Confidential



TG 2

Arwen Smits
Danny Van Hemelrijck





1. Introduction

This report contains the test results, graphs and photos from preliminary static biaxial tests on cruciform specimens carried out at the Department of Mechanics of Materials and Constructions of the VUB within the framework of the Optimat Blades project. It consists of 10 preliminary tests: 10 tests on two different specimen geometries. The first specimen geometry has at the intersection of the arms a radius of curvature equal to 10 mm; the other geometry has a radius equal to 20 mm. For the two specimen geometries three tensile tests were performed with loading ratio $F_x/F_y = 2.2/1$ and 2 tests with loading ratio $F_x/F_y = 4.4/1$ in tension. Direction x or direction 0° is the direction of the UD fibers.

2. Material and specimens

The test coupons are made of MD material with $([\pm 45^\circ, 0^\circ]_3, [\pm 45^\circ])$ -lay-up and are delivered by LM Glasfiber A/S Denmark. The lay-up is not completely symmetric since $+45^\circ$ layer and -45° layer are always placed in the same sequence. The geometry of the cruciform specimens is shown in Figure 1. The width in the direction of the UD fibres (0° direction) is 20 mm; the width in the perpendicular direction is 25 mm. This difference in width is used to be sure the test bench is able to reach the failure load in 0° direction and to have a test section as large as possible. Two specimen geometries with at the intersection of two arms a radius of curvature R equal to 10 mm and 20 mm were tested. The thickness of the specimens in the test zone is about 5.08 mm.

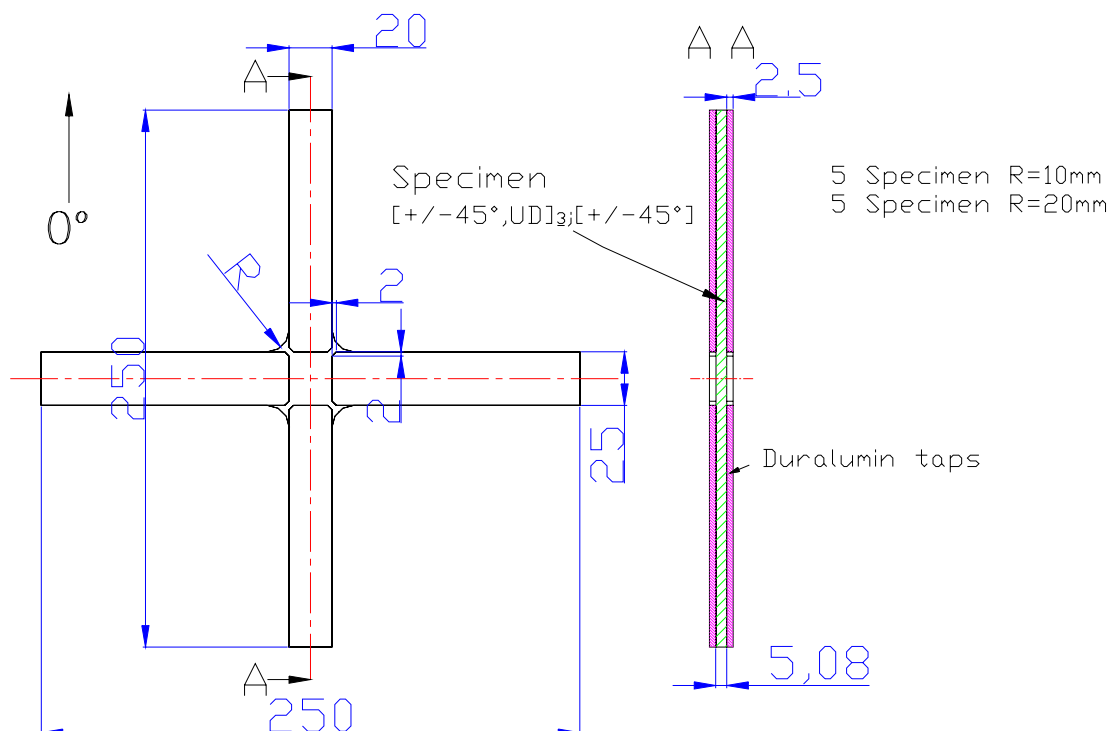


Figure 1: Geometry of cruciform specimens.



3. Test set-up

All specimens were tested in tension/tension using a servo-hydraulic biaxial test bench with a loading capacity of 100 kN in both directions (Figure 2). In the measurement zone of each specimen a rosette type strain gauge was bonded on both sides with P2 adhesive. Strain measurements are obtained in 0° direction (direction of UD fibers), 90° direction (perpendicular to UD fibers) and in 45° direction. The strain gauges are from Tokyo Sokki Kenkyujo Co., Ltd. The strain gauge type is FRA – 3: the gauge factor is 2.09, the gauge length is 3 mm and the gauge width is 1.8 mm. A digital video camera was used during testing to allow for specimen failure visualization.

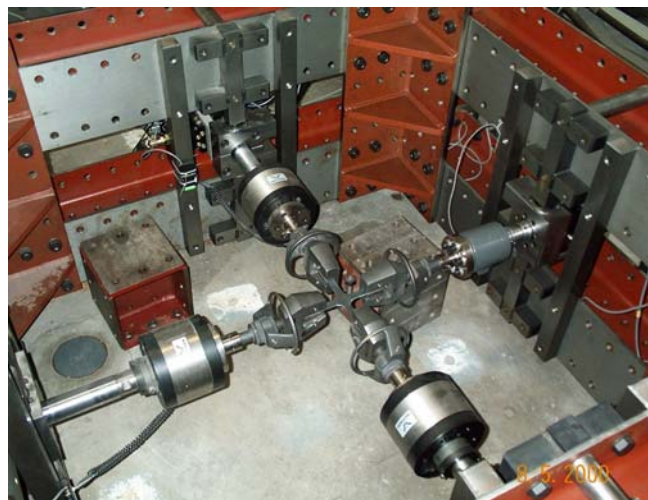


Figure 2: Biaxial test bench for cruciform specimens.

4. Test graphs and photos

For each test 3 photos are shown from the beginning of failure until the final failure. The OW direction on the photos is the direction of the UD fibers at 0° and NZ direction is the perpendicular direction. Four test cases are shown: loading ratios 2.2/1 and 4.4/1 for the curvature R=10 mm and R=20 mm.

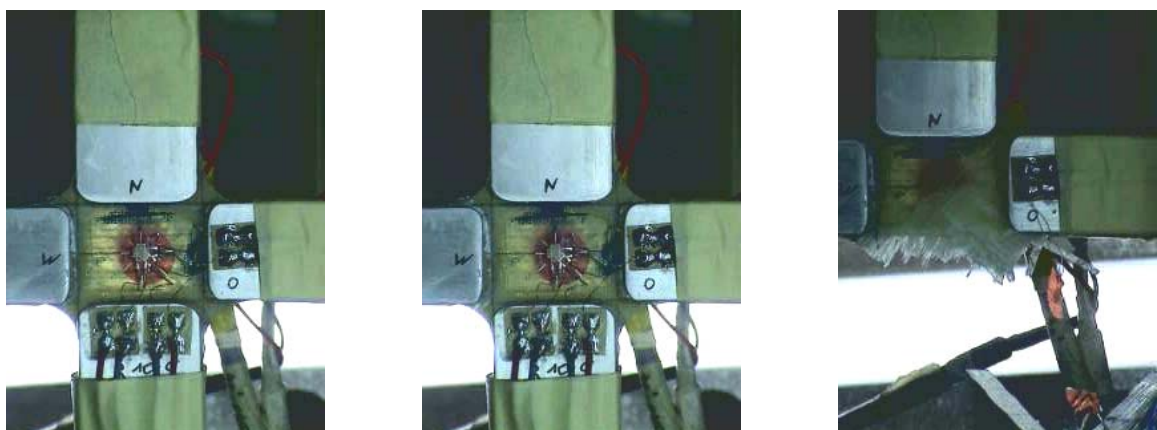


Figure 3: Photos of specimen R 10 C, Loading ratio=2.2/1.

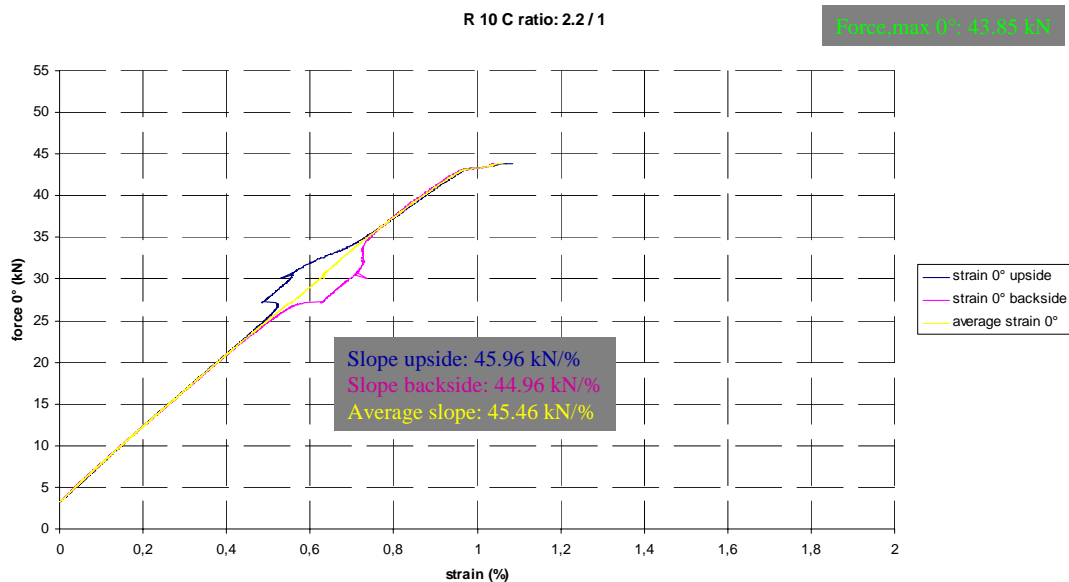


In addition to the three photos, three graphs are shown for each test. The first graph contains the applied load in the 0° direction vs. the strain in that direction. The second graph shows the load in the 90° direction vs. the strain in that direction and the last graph shows the load in the 0° direction vs. strain in 45° direction. In each graph three curves are drawn. The blue one is for the strain gauge at the upper side of the specimen, the red one at the backside of the specimen and the yellow one gives the average values.

First photo's and graphs are for specimen R 10 C loaded at ratio 2.2/1.

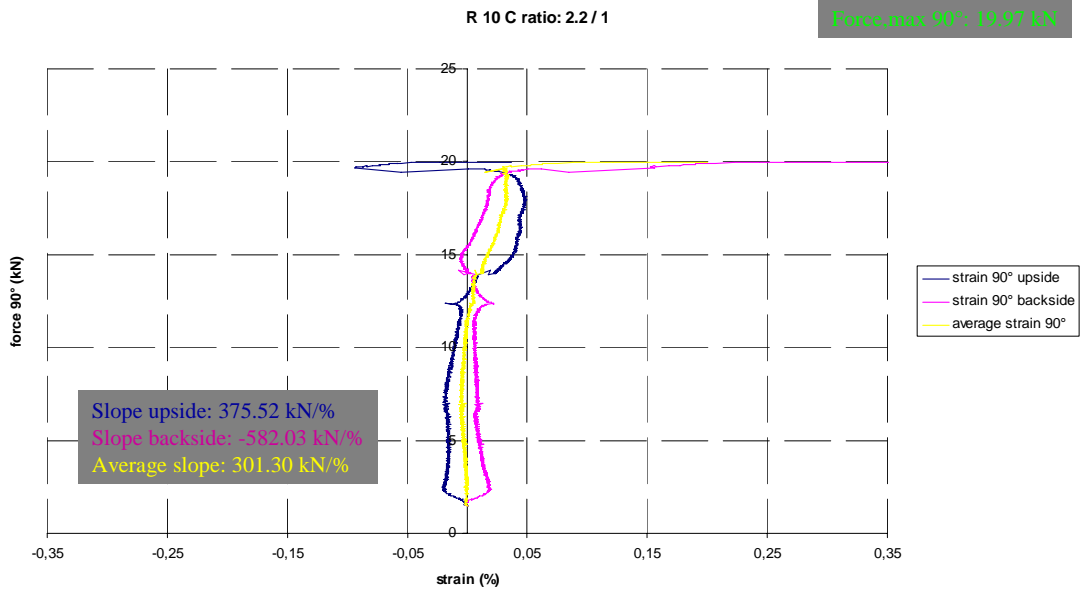
For specimen R 10 C failure started at the intersection between (see photos) the south arm and the west arm after the end-taps in 0° direction debonded at about 27kN. The jump in the strains shown in graph 1a, is due debonding of the end-taps. Also the end-taps in the 90° direction debonded. Next, cracks appeared at the corner between the south arm and the east arm and finally the south arm was pulled off.

The strains and slopes at both sides of the specimen are comparable in the 0° direction as can be seen on graph 1 a.



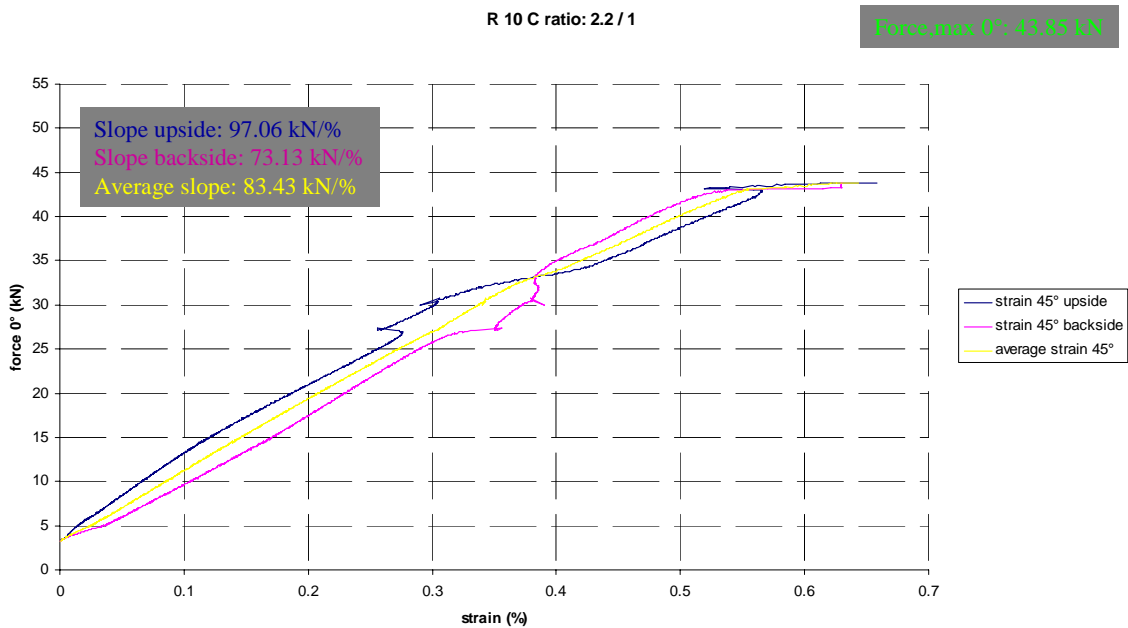
Graph 1a: Load in 0° direction vs. strain in 0° direction. R=10mm, Loading ratio=2.2/1.

Due to debonding of the strain gauges just before final failure the strains at the end of the test are not valid. This is only at the end of the test at loads close to the failure load (at 43kN in 0° direction and 19kN in 90° direction). This is certainly the case at the end of the curves in graph 1 b, showing the strains and forces in the 90° direction.



Graph 1b: Load in 90° direction vs. strain in 90° direction. R=10mm, Loading ratio=2.2/1.

The strains in the 90° direction are about zero and are quite different at both sides of the specimen as shown on graph 1 b. The jumps in strain in the loading area from 13 kN till 14.5 kN are due to debonding of the end-taps. For the jump at the beginning of the test and for the strange progress of the curves we haven't found a suitable explanation yet. The strains at the upper side of the specimen are increasing with increasing load while the strains at the backside are decreasing and become negative. The difference between upper side and backside can partly be due to the asymmetric lay-up of the MD material. The slopes are taken between 5kN and 10kN in the 90° direction.



Graph 1c: Load in 0° direction vs. strain in 45° direction. R=10mm, Loading ratio=2.2/1.



The strains in the 45° direction are quite linear until the end-taps start to debond at loads of 27kN in the 0° direction. The difference in slopes and strains between upper side and backside of the specimens are not completely clear but might partially explained by the asymmetric lay-up of the MD material for the specimens.

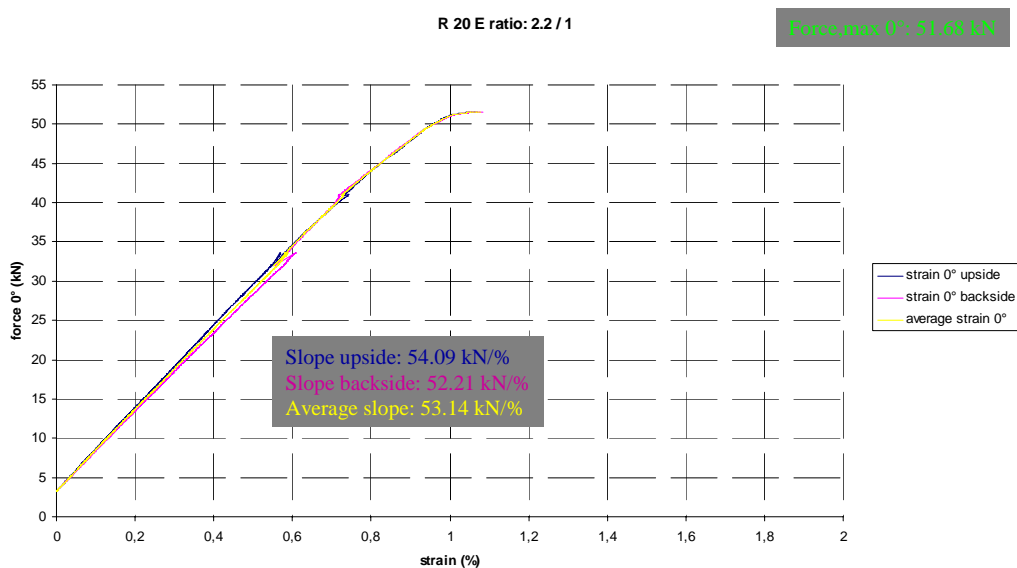
Next photo's and graphs show the specimen R 20 E loaded at ratio 2.2/1.



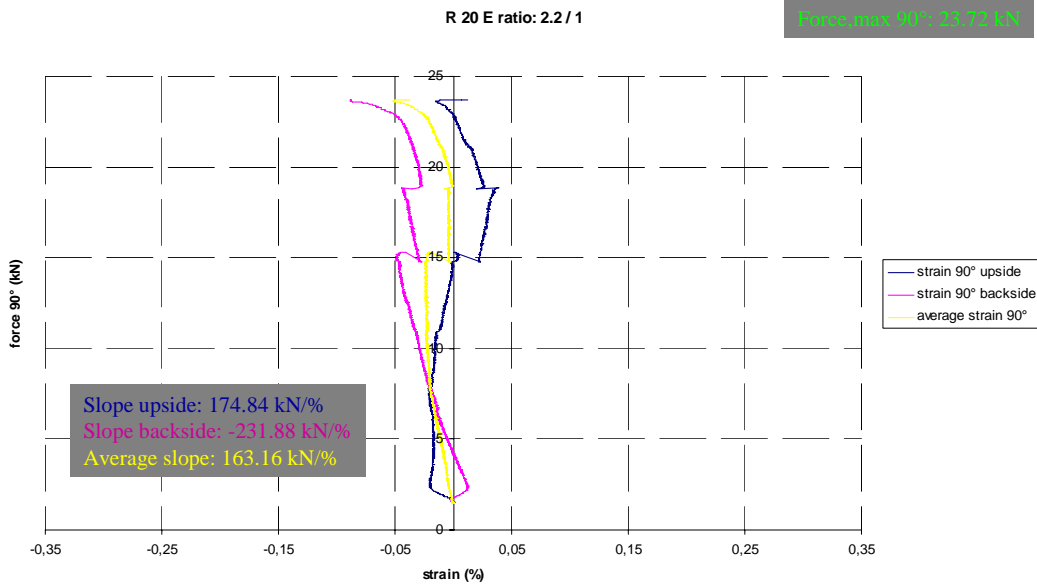
Figure 4: Photos of specimen R 20 E, Loading ratio=2.2/1.

Specimen R 20 E started failing near the intersection between the arms called north and west on the photos and after debonding of the end-taps in 0° direction at about 33kN and in the perpendicular direction at 41kN. Finally arm south was pulled off.

The strains and slopes at both sides of the specimen are comparable in the 0° direction as can be seen on graph 2 a. The slopes are higher than in specimen R 10 C where the slopes have a value of about 45kN/%. The failure forces are higher.

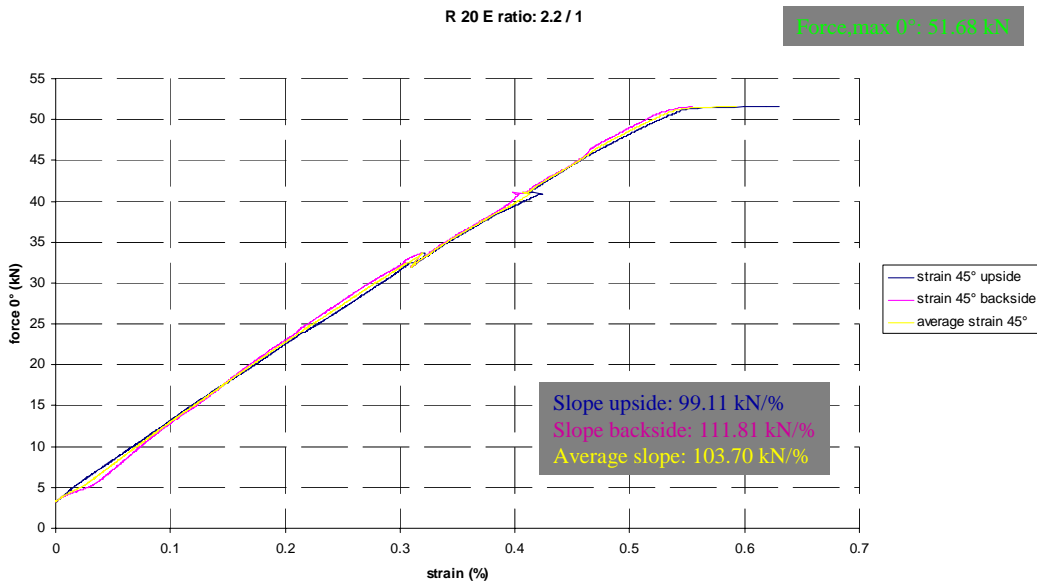


Graph 2a: Load in 0° direction vs. strain in 0° direction. R=20mm, Loading ratio=2.2/1.



Graph 2b: Load in 90° direction vs. strain in 90° direction. R=20mm, Loading ratio=2.2/1.

For the results in the 90° direction we see the same strange effects as for specimen R 10 C. The strains at the upper side of the specimen are increasing with increasing load while the strains at the backside are decreasing and become negative.



Graph 2c: Load in 0° direction vs. strain in 45° direction. R=20mm, Loading ratio=2.2/1.

The strains in the 45° direction are linear until end-tap failure at loads of 33kN, for end-tap west and east failure occurred around 41kN. This can be seen on graph 2 c as jumps in the strains at these loads. The differences in slopes between upper side and backside are lower than in specimen R 10 C and the global values are higher.



Next range of photo's and graphs is for specimen R 10 D loaded at ratio 4.4/1.

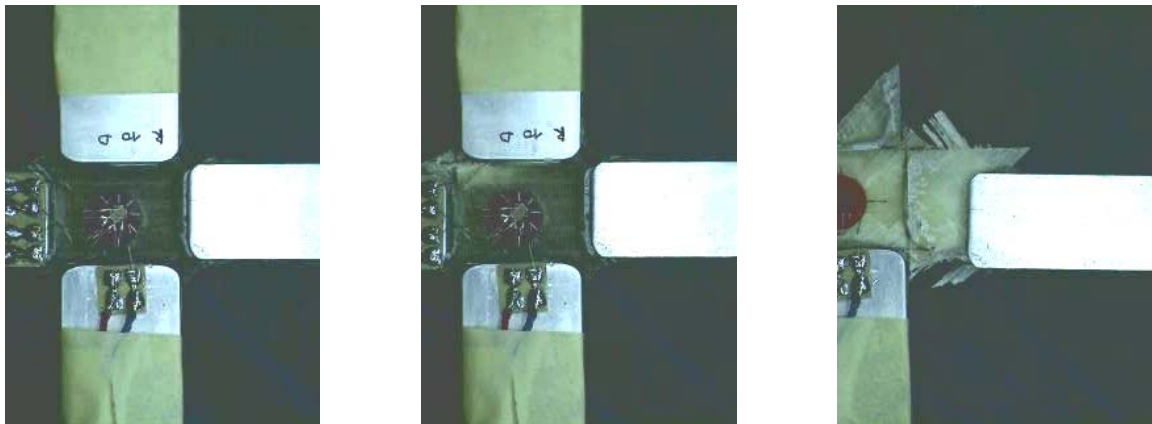
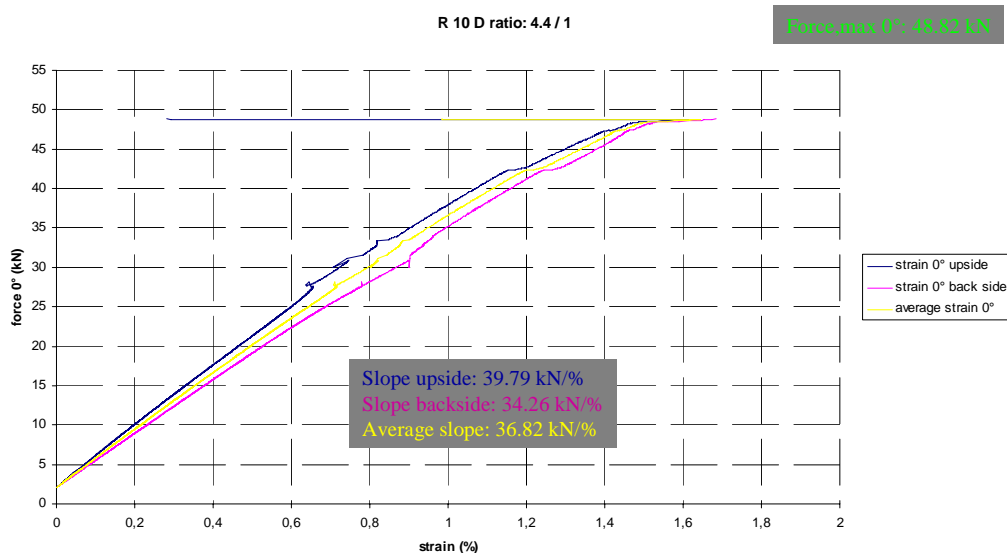


Figure 5: Photos of specimen R 10 D, Loading ratio=4.4/1.

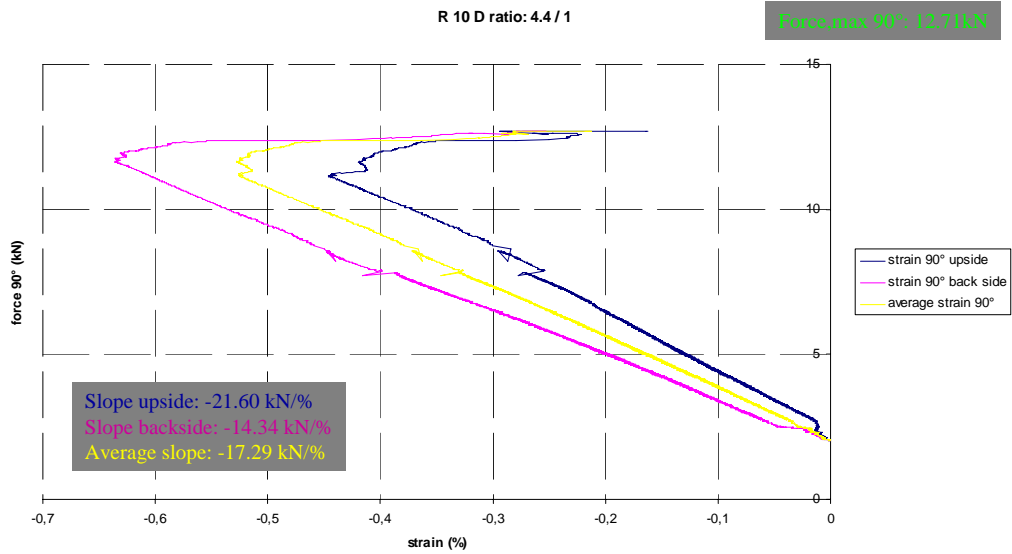
For specimen R 10 D the end-tab on the west arm debonded first, then the end tab on the east arm. Cracks between arm north and west appeared afterwards and finally arm north was pulled off together with failure in the east arm.

Graph 3a shows the strains and loads in the 0° direction. There's a difference in slopes between the upper side and backside of the specimen and slopes are lower compared to the specimens loaded with ratio 2.2/1. When the load ratio is equal to 4.4/1 compared to 2.2/1 the load in the perpendicular direction (90°) is relatively lower, in fact 2 times lower for the same load in the 0° direction. Consequently with the load ratio equal to 4.4/1 the strain in the 0° direction will be less reduced due to the Poisson effect, resulting in a lower slope.



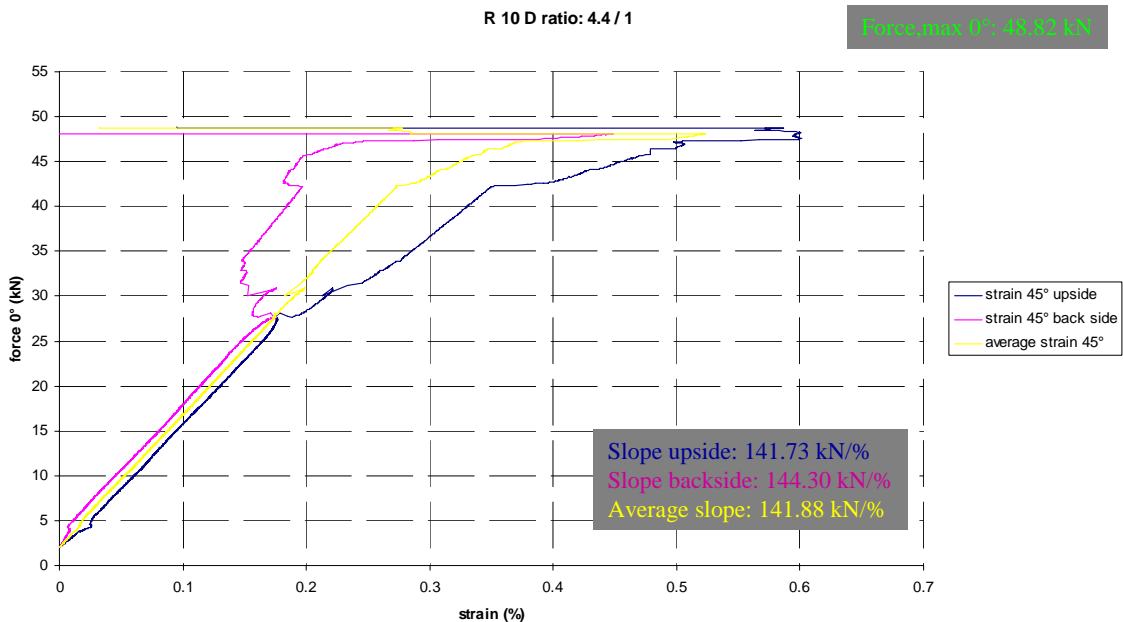
Graph 3a: Load in 0° direction vs. strain in 0° direction. R=10mm, Loading ratio=4.4/1.

Strains at the end of the test are not valid since strain gauges debonded before the end of the test. This is at loads of 47kN in 0° direction and 12.5kN in 90° direction.



Graph 3b: Load in 90° direction vs. strain in 90° direction. R=10mm, Loading ratio=4.4/1.

On graph 3b we can see the slopes in the 90° direction being completely negative. This is due to relative high applied loads in the 0° direction combined with high Poisson coefficients. The differences in slopes between upper side and backside of the specimen are quite high. Also the jump in strains at the beginning of the test is rather strange.



Graph 3c: Load in 0° direction vs. strain in 45° direction. R=10mm, Loading ratio=4.4/1.

Strain data in the 45° direction are only valid until loads equal to 28kN in the 0° direction since then end-taps started to debond. The slopes are higher compared to specimens loaded at ratio 2.2/1.



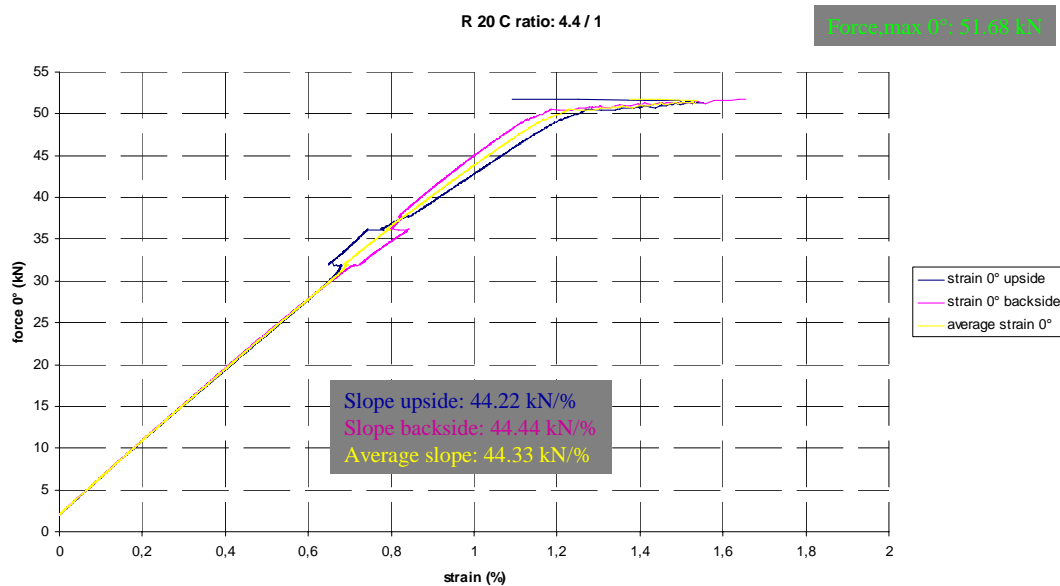
Last range of photo's and graphs show the specimen R 20 C loaded at ratio 4.4/1.



Figure 6: Photos of specimen R 20 C, Loading ratio=4.4/1.

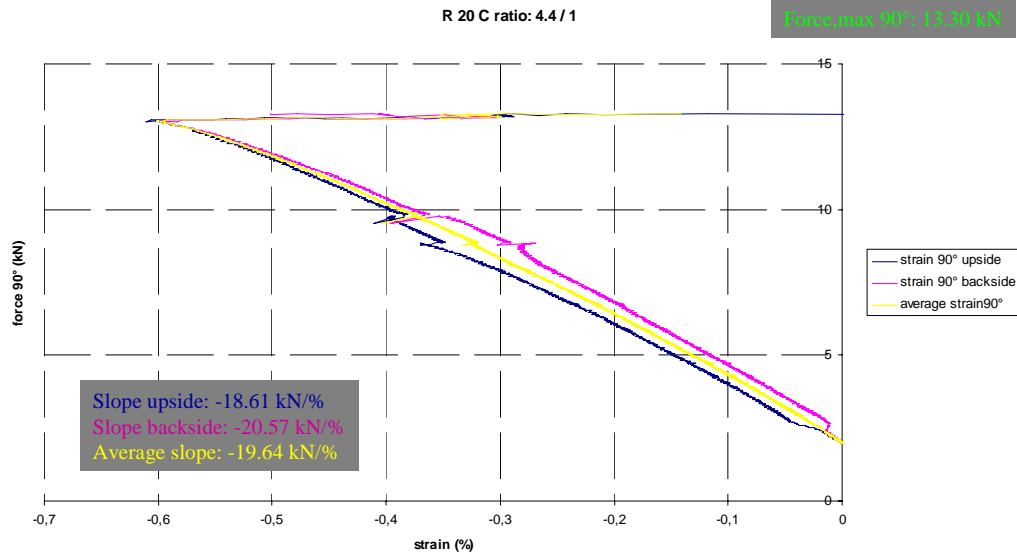
For specimen R 20 C end-tap west debonded at a load of 32kN in the 0° direction and end-tap east at 37kN as can be seen on graph 4a as jumps in the strains. Then cracks between arm north and west occurred and finally arm west was broken.

The strains and slopes at both sides of the specimen are comparable in the 0° direction. The slopes are higher than in specimen R 10 D where the slopes have a value of about 37kN. The failure forces are higher.



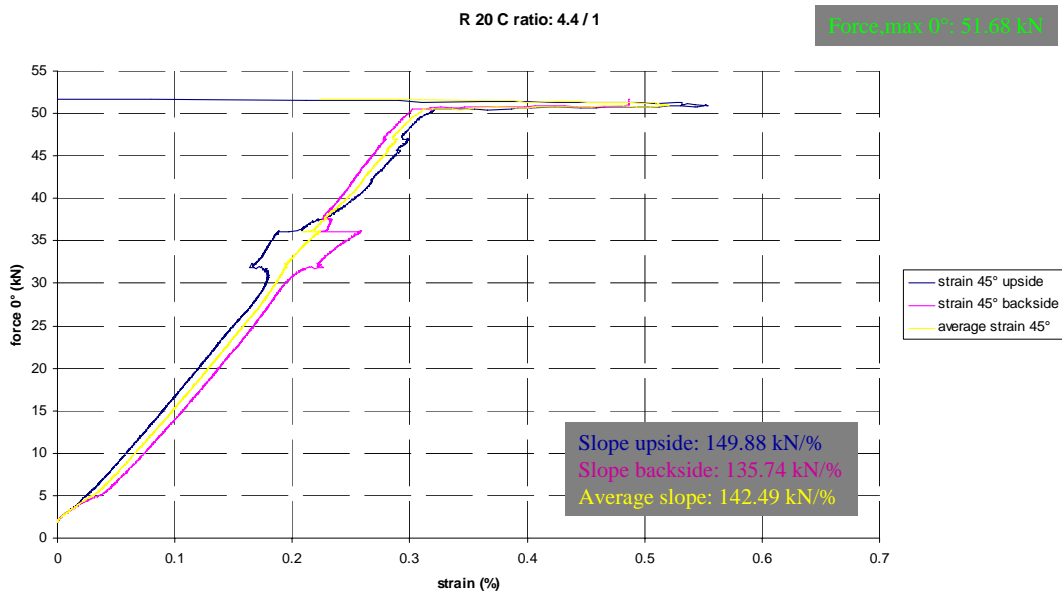
Graph 4a: Load in 0° direction vs. strain in 0° direction. R=20mm, Loading ratio=4.4/1.

At loads equal to 50kN in the 0° direction and 12.5kN in the 90° direction strain gauges debonded.



Graph 4b: Load in 90° direction vs. strain in 90° direction. R=20mm, Loading ratio=4.4/1.

Graph 4b shows negative slopes in the 90° direction. The differences in slopes between upper side and backside of the specimen are not as high as in specimen R 10 D. Again there's a jump in strains at the beginning of the test.



Graph 4c: Load in 0° direction vs. strain in 45° direction. R=20mm, Loading ratio=4.4/1.

For all specimens, at loads of about 30kN in the 0° direction, the end-taps in that direction started to debond. Afterwards, for some specimens the end-taps in the 90° direction also debonded. Both facts occur at loads far under the failure load of the specimens so the design of the end-taps should certainly be reconsidered. Failure of the majority of the specimens started at one of the intersections between the two arms; other specimens failed in one of the arms itself after debonding of the end-taps.



5. Overview of test results

Table 1 gives an overview of obtained maximum loads in 0° direction and 90° direction and a description of the observed failure modes. Failure stresses are not given since they can't be directly calculated from the applied forces, as the area taking the applied load is not known. The direction of the UD fibers is the 0° direction or east-west direction. The applied loads in both directions are automatically connected to each other by the loading ratio (2.2/1 or 4.4/1). The highest load is applied in the 0° direction. As failure didn't start from the middle of the test zone but from the intersection of the arms, no actual biaxial failure was obtained and results should be interpreted carefully. However if the obtained values are comparable to uniaxial failure stresses, the results can be considered as valid. For the moment no uniaxial test results are available for comparison. The specimens are numbered from A to E for each design. R 10 and R 20 are the names for a design with radius of curvature R=10 mm and R=20 mm respectively.

As can be seen in table 1 R= 10 mm gives lower failure forces in the 0° direction for loading ratio $F_x/F_y = 2.2/1$ (average about 41kN) compared to R= 20 mm (average about 51kN). For loading ratio $F_x/F_y = 4.4/1$ the obtained failure forces in the 0° direction are almost the same for both curvatures. The failure modes for all specimens are almost the same. First end-tap debonding occurs, then cracks between to arms are formed and finally failure of one of the arms.

		force 0° max (kN)	force 90° max (kN)	failure mode
R 10 A	ratio: 0° / 90°=2.2 / 1	40.05	18.63	n-tap east, n-tap west, arm north broken
R 10 B	ratio: 0° / 90°=2.2 / 1	38.40	17.95	n-tap west, n-tap east, cracks between arm north and west, arm north broken
R 10 C	ratio: 0° / 90°=2.2 / 1	43.85	19.97	n-tap west, n-tap east, n-tap north, cracks between arm south and west, cracks between arm south and east, arm south broken
R 10 D	ratio: 0° / 90°=4.4 / 1	48.82	12.71	n-tap west, n-tap east, cracks between arm north and west, arm north broken
R 10 E	ratio: 0° / 90°=4.4 / 1	52.67	12.04	n-tap west + east at 30kN, cracks between arm south and west, arm south broken together with arm east
	average 2.2 / 1:	40.77	18.85	
	average 4.4 / 1:	50.74	12.37	
R 20 A	ratio: 0° / 90°=2.2 / 1	52.11	24.15	n-tap west, n-tap east, cracks between arm south and east, diagonal cracks in front of arm south, arm west broken
R 20 B	ratio: 0° / 90°=2.2 / 1	49.66	23.11	n-tap east, n-tap west, cracks between arm south and east, arm south broken, arm east broken
R 20 C	ratio: 0° / 90°=4.4 / 1	51.68	13.30	n-tap west + east at 37kN, cracks between arm north and west, arm west broken
R 20 D	ratio: 0° / 90°=4.4 / 1	47.47	12.38	n-tap west + east, cracks between arm north and west, arm north almost broken, diagonal crack from north-west to south-east
R 20 E	ratio: 0° / 90°=2.2 / 1	51.58	23.72	n-tap west and east at 33kN, n-tap north and south at 41kN, cracks between arm north and west, arm north broken
	average 2.2 / 1:	51.12	23.66	
	average 4.4 / 1:	49.58	12.84	

Table 1: Failure loads in 0° direction and 90° direction and failure modes.

Table 2 gives an overview of obtained slopes in 0° direction. The slopes are calculated using linear regression for the applied load in the 0° direction ranging between 5kN and 10 kN and the measured strains (upper side of specimen, backside and average) in the same direction. The obtained slopes have the dimension of [kN/%] and can't be considered as real stiffness values since no stresses can be calculated out of the applied forces.



R 10		Slope 0°		
		up	back	average
R 10 A	ratio: 0° / 90°=2.2 / 1	39.84	46.24	42.81
R 10 B	ratio: 0° / 90°=2.2 / 1	39.46	45.85	42.42
R 10 C	ratio: 0° / 90°=2.2 / 1	45.96	44.96	45.46
	average 2.2 / 1:	41.75	45.68	43.56
R 10 D	ratio: 0° / 90°=4.4 / 1	39.79	34.26	36.82
R 10 E	ratio: 0° / 90°=4.4 / 1	37.47	40.56	38.96
	average 4.4 / 1:	38.63	37.41	37.89
R 20				
R 20 A	ratio: 0° / 90°=2.2 / 1	54.28	55.60	54.95
R 20 B	ratio: 0° / 90°=2.2 / 1	49.83	68.16	57.58
R 20 E	ratio: 0° / 90°=2.2 / 1	54.09	52.21	53.14
	average 2.2 / 1:	52.73	58.66	55.22
R 20 C	ratio: 0° / 90°=4.4 / 1	44.22	44.44	44.33
R 20 D	ratio: 0° / 90°=4.4 / 1	43.32	45.66	44.46
	average 4.4 / 1:	43.77	45.05	44.39

Table 2: Slopes in 0° direction.

R= 10 mm gives lower slopes for both loading ratio's than R= 20 mm. For loading ratio 2.2/1 the obtained slopes are about 43.6kN/% for R=10 mm and about 55.2kN/% for R=20 mm; for loading ratio 4.4/1 the obtained slopes are about 37.9kN/% for R=10 mm and about 44.4kN/% for R = 20 mm. For loading ratio 2.2/1 the slopes are higher than for loading ratio 4.4/1. This is logical since for loading ratio 2.2/1 more force is relatively applied in the perpendicular direction. This results in higher strains in the 90° direction and so to higher Poisson effects in the 0° direction.

Table 3 gives an overview of obtained slopes in the 90° direction. The slope is calculated using the applied load in the 90° direction between 5kN and 10 kN and the measured strains in the same direction.

R 10		Slope 90°		
		up	back	average
R 10 A	ratio: 0° / 90°=2.2 / 1	-100.46	91.58	168.84
R 10 B	ratio: 0° / 90°=2.2 / 1	180.49	-190.81	80.24
R 10 C	ratio: 0° / 90°=2.2 / 1	375.52	-582.03	301.30
	average 2.2 / 1:	151.85	-227.08	183.46
R 10 D	ratio: 0° / 90°=4.4 / 1	-21.60	-14.34	-17.29
R 10 E	ratio: 0° / 90°=4.4 / 1	-16.25	-16.54	-16.42
	average 4.4 / 1:	-18.92	-15.44	-16.85
R 20				
R 20 A	ratio: 0° / 90°=2.2 / 1	-181.00	319.10	-339.17
R 20 B	ratio: 0° / 90°=2.2 / 1	-120.60	27.08	-193.10
R 20 E	ratio: 0° / 90°=2.2 / 1	174.84	-231.88	163.16
	average 2.2 / 1:	-42.25	38.10	-123.03
R 20 C	ratio: 0° / 90°=4.4 / 1	-18.61	-20.57	-19.64
R 20 D	ratio: 0° / 90°=4.4 / 1	-15.83	-17.99	-16.89
	average 4.4 / 1:	-17.22	-19.28	-18.27

Table 3: Slopes in 90° direction.



For loading ratio 2.2/1 the obtained strains are almost zero and so the slopes are very high. Some slopes are negative, others are positive. That is why taking average values doesn't make much sense. Some strains increase while loading, other strains decrease. For loading ratio 4.4/1 the obtained strains are all negative and they all decrease while loading. This is due to the high loading in the 0° direction and the high Poisson coefficient.

Table 4 gives an overview of obtained slopes in 45° direction. The slope is calculated using the applied load in the 0° direction between 5kN and 10 kN and the measured strains in the 45° direction.

R 10	Slope 45°			
		up	back	average
R 10 A	ratio: 0° / 90°=2.2 / 1	95.89	117.34	105.02
R 10 B	ratio: 0° / 90°=2.2 / 1	52.47	201.50	83.66
R 10 C	ratio: 0° / 90°=2.2 / 1	97.06	73.13	83.43
	average 2.2 / 1:	81.81	130.66	90.70
R 10 D	ratio: 0° / 90°=4.4 / 1	141.73	144.30	141.88
R 10 E	ratio: 0° / 90°=4.4 / 1	112.78	310.87	165.79
	average 4.4 / 1:	127.26	227.59	153.83
R 20				
R 20 A	ratio: 0° / 90°=2.2 / 1	138.56	99.85	113.46
R 20 B	ratio: 0° / 90°=2.2 / 1	91.01	95.76	91.85
R 20 E	ratio: 0° / 90°=2.2 / 1	99.11	111.81	103.70
	average 2.2 / 1:	109.56	102.47	103.00
R 20 C	ratio: 0° / 90°=4.4 / 1	149.88	135.74	142.49
R 20 D	ratio: 0° / 90°=4.4 / 1	186.72	203.61	194.89
	average 4.4 / 1:	168.30	169.67	168.69

Table 4: Slopes in 45° direction.

R=10 mm gives lower slopes for both loading ratio's compared to R=20 mm. For loading ratio 2.2/1 the obtained slopes are about 91kN/% for R=10 mm and about 103kN/% for R=20 mm; for loading ratio 4.4/1 the obtained slopes are about 154kN/% for R=10 mm and about 169kN/% for R=20 mm. The slopes are much lower for loading ratio 2.2/1 than for loading ratio 4.4/1. At loading ratio 2.2/1 the combined load is more applied in the direction of the +/-45° fibers than at loading ratio 4.4/1 and so the strains are higher in the +/-45° direction at loading ratio 2.2/1.

All specimens were placed in the test bench with the exterior + 45° fibers at the upper side and the exterior - 45° at the backside. The strain gauges however were not always placed in the same manner. Sometimes the strain gauges in the 45° direction were placed in the same direction as the fibers at the exterior side and sometimes at the opposite direction. An overview is given in table 5. This can also explain differences in test results.



	direction strain gauge 45°		direction fibers 45° at surface		conclusion direction	
	upper side	backside	upper side	backside	upper side	backside
R 10 A	+45° (NO)	-45° (NW)	+45° (NO)	-45° (NW)	same direction	same direction
R 10 B	-45° (NW)	+45° (NO)	+45° (NO)	-45° (NW)	opposite direction	opposite direction
R 10 C	-45° (NW)	+45° (NO)	+45° (NO)	-45° (NW)	opposite direction	opposite direction
R 10 D	+45° (NO)	-45° (NW)	+45° (NO)	-45° (NW)	same direction	same direction
R 10 E	+45° (NO)	-45° (NW)	+45° (NO)	-45° (NW)	same direction	same direction
R 20 A	-45° (NW)	+45° (NO)	+45° (NO)	-45° (NW)	opposite direction	opposite direction
R 20 B	-45° (NW)	+45° (NO)	+45° (NO)	-45° (NW)	opposite direction	opposite direction
R 20 C	-45° (NW)	+45° (NO)	+45° (NO)	-45° (NW)	opposite direction	opposite direction
R 20 D	+45° (NO)	-45° (NW)	+45° (NO)	-45° (NW)	same direction	same direction
R 20 E	-45° (NW)	+45° (NO)	+45° (NO)	-45° (NW)	opposite direction	opposite direction

Table 5: Position of 45° strain gauges in comparison with fiber direction.

6. Conclusions

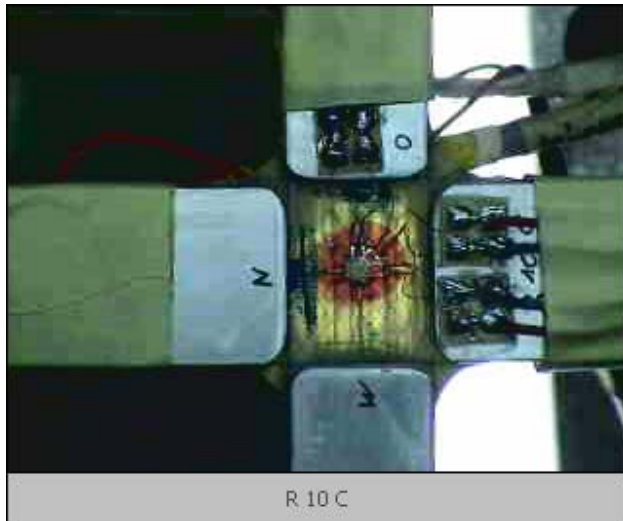
To be considered a valid biaxial test, different objectives are to be met: (i) a uniform stress distribution in the gauge section, which should be large enough to put a strain gauge or extensometer and (ii) ultimate specimen failure must be initiated in or around the gage section of the test specimen. For the majority of the specimens, failure started at one of the intersections between two arms and therefore the test results can't be considered as real biaxial test results. The obtained results should therefore be compared with failure load results on uniaxially loaded specimens. If the values are comparable, the obtained biaxial test results can be considered as good test results. New proposals for the specimen geometry should be made.

7. Proposals for new geometry

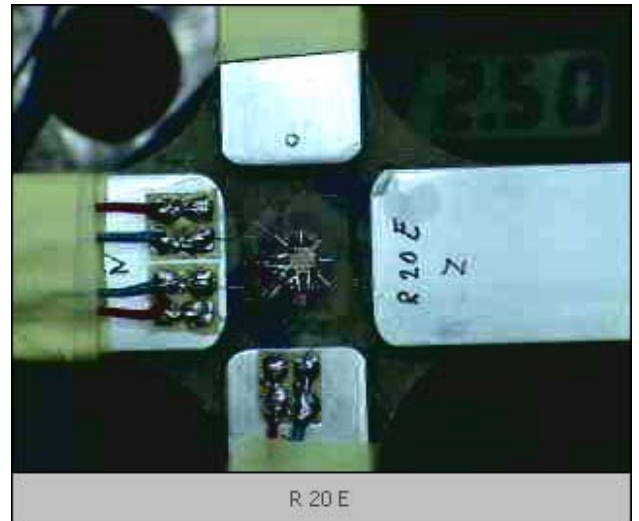
All new specimens will have the same width of 25 mm in both directions since no problems were encountered with the inability to failure the specimens only values of +/- 50kN were necessary to obtain failure. The values of the failure load will probably be higher when failure occurs in the test zone compared to failure in one of the arms after end-tap debonding. However, loads of more than 100kN (the capacity of the biaxial test bench) will not be obtained. A radius of curvature R=20 mm will be used for the new specimens since this value gave less stress concentrations in the intersection zone of two arms compared to R=10 mm. As early failure of the end taps occurred for each load case, the end taps should certainly be adapted. First the original duralumin taps will be tapered. In the next step for lowering the interlaminar stresses the end taps will be made in glass fibre epoxy. The third step is not to use end-taps anymore but to mill material carefully away in the test zone.



8. Video's of tests



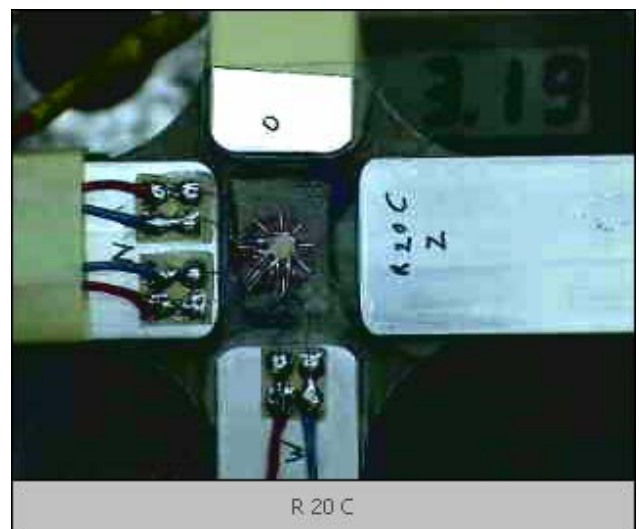
a) R = 10 mm, ratio: 2.2/1



b) R = 20 mm, ratio: 2.2/1



c) R = 10 mm, ratio: 4.4/1



d) R = 20 mm, ratio: 4.4/1